Electronic Supplementary Information for

Defect evolution behaviors from single sulfur point vacancies to line vacancies in the monolayer molybdenum disulfide

Chan Gao[1,2], Xiaoyong Yang[3], Ming Jiang[1], Lixin Chen[1], Zhiwen Chen[1], Chandra Veer Singh[1,4,*]

[1]*Department of Materials Science and Engineering, University of Toronto, Toronto, ON M5S 3E4, Canada*

[2]*Institute of Nuclear Physics and Chemistry, China Academy of Engineering Physics, Mianyang 621900, China*

[3]*Condensed Matter Theory Group, Materials Theory Division, Department of Physics and Astronomy, Uppsala University, Uppsala 75120, Sweden*

[4]*Department of Mechanical and Industrial Engineering, University of Toronto, Toronto, ON M5S 3G8, Canada*

* Correspondence and request for materials should be addressed to C.V. Singh (chandraveer.singh@utoronto.ca).

S1 Basic properties of monolayer MoS_2

The zero-temperature equilibrium lattice constant and cohesive energy of unit cell were calculated by minimizing the energy of monolayer MoS_2 using conjugate gradients with force and energy tolerances of 10^{-10} eV/Å and 10^{-10} eV, respectively[1].

The structural stability of monolayer MoS_2 with vacancy defects can be studied by the formation energy, i.e., the amount of energy required to remove atoms. The formation energy per vacancy E_{form} in the defective monolayer MoS_2 can be obtained using the following equation[2]:

$$E_{form} = \frac{E_{defect} - E_{pristine} + N_i \mu_i}{N_i} \tag{1}$$

where E_{defect}, $E_{pristine}$ are the total energy of the defective monolayer and pristine monolayer MoS_2, respectively, and μ_i is the chemical potential of Mo or S, depending on the type of defect in monolayer MoS_2 with N_i vacancies. The chemical potentials of Mo and S atoms are obtained from body centered cubic (BCC) bulk molybdenum and the stable S_8 ring, respectively. The computed chemical potentials of Mo and S atoms using DFT were -10.93 and -4.13 eV, respectively, which agree well with the corresponding previous results of -11.09 and -4.03 eV[3]. The formation energy of vacancies depends highly on the concentration of vacancies in the materials. The sizes of the system that generates the vacancies in Figure S1 are 5 × 5 supercell and 2.55 nm × 2.76 nm ($8a_0 \times 5\sqrt{3}a_0$, a_0 is the lattice parameter) for the first principles and molecular dynamics calculations, respectively.

S2 Mechanical properties of monolayer MoS_2

Due to D_{3h} symmetry, there are only two independent elastic constants C_{11} and C_{12}, and C_{11} and C_{22} are the same, which means that the orientation (the armchair and zigzag direction) does not affect the elastic behavior of monolayer MoS_2 under small strain. The zero-temperature linear elastic constants C_{11} and C_{12} are calculated using molecular

statics simulation by finite difference[1, 4],

$$C_{11} = \frac{\Delta\sigma_1}{\Delta\varepsilon_1} \tag{2}$$

$$C_{12} = \frac{1}{2}\left(\frac{\Delta\sigma_1}{\Delta\varepsilon_2} + \frac{\Delta\sigma_2}{\Delta\varepsilon_1}\right) \tag{3}$$

$$C_{66} = \frac{1}{2}(C_{11} - C_{12}) \tag{4}$$

where $\Delta\sigma$ and $\Delta\varepsilon$ are the stress and strain induced by infinitesimally changing simulation box from their equilibrium state, respectively.

Theoretically, the isotropic linear elastic properties, the in-plane Young's modulus E and Poisson's ratio ν can be calculated as[4]:

$$E = (C_{11}^2 - C_{12}^2)/C_{11} \tag{5}$$

$$\nu = C_{12}/C_{11} \tag{6}$$

The elastic constants of monolayer MoS2 with defects depend on the defect concentration. The size of monolayer MoS_2 was taken as $5a_0 \times 3\sqrt{3}a_0$ with a line vacancies defect along x zigzag direction and single point vacancy defects, where a_0 is the lattice parameter. It should be noted that C_{11} is not equal to C_{22} in the monolayer MoS2 with defects.

S3 Ultimate strain and strength of monolayer MoS2 with defects

In order to study the effects of the sulfur point vacancies and line vacancies defects on the ultimate strain and strength of monolayer MoS2, the same calculation method as in the main text was used. The size of monolayer MoS_2 was taken as 3.1 nm × 3.2 nm ($10a_0 \times 6\sqrt{3}a_0$, a_0 is the lattice parameter) with a line vacancies defect along x zigzag direction and single point vacancy defects with the same number of sulfur vacancies,

as shown in Figure S4.

Table S1. Lattice parameter (a_0), Mo-S bond distance ($d_{Mo\text{-}S}$), the distance between the two nearest S atoms above and below the Mo layer ($d_{S\text{-}S}$), the cohesive energy per unit cell (E_c), the formation energy of S vacancy (E_S) and Mo vacancy (E_{Mo}) of monolayer MoS_2 calculated by DFT and MD with different interatomic potentials.

Potential	a_0	$d_{Mo\text{-}S}$	$d_{S\text{-}S}$	E_c (eV)	E_S (eV)	E_{Mo} (eV)
DFT	3.18424	2.41248	3.12427	-21.84638	2.6476	7.16797
SW13	3.06430	2.39820	3.23814	-12.77177	3.84034	6.21984
SW13_f	3.09368	2.39204	3.18217	-12.75808	3.83076	6.22058
SW15	3.11754	2.38115	3.11781	-3.716560	--	--
REBO	3.16752	2.44393	3.24248	-21.48697	3.59333	6.08057
SW16	3.19757	2.46094	3.25458	-8.80474	1.80083	6.79146
ReaxFF	3.18605	2.43248	3.18328	-15.13643	2.68602	8.08712

Table S2. Energy differences between monolayer MoS_2 with a line defect and single point vacancy defects with 2 (ΔE_2) and 3 (ΔE_3) sulfur vacancies calculated by DFT and MD with different interatomic potentials, where $\Delta E = \Delta E_{point} - \Delta E_{line}$.

Potential	ΔE_2	ΔE_3
DFT	0.06452	0.08822
SW13	0.15200	0.31634
SW13_f	0.13720	0.27932
SW15	0.0	0.0
REBO	0.12024	0.28015
SW16	0.24286	0.54568
ReaxFF	0.11532	0.24667

Table S3. The elastic constants C_{11}, C_{12} and C_{66}, Young's modulus E and Poisson's ratio v of monolayer MoS_2 calculated by DFT and MD with different interatomic potentials.

Potential	C_{11} (N/m)	C_{12} (N/m)	C_{66} (N/m)	E (N/m)	ν
DFT	133.761	32.953	50.404	125.643	0.246
SW13	81.775	30.168	25.80352	70.646	0.369
SW13_f	140.774	52.735	44.018	121.019	0.375
SW15	105.331	28.299	38.514	97.728	0.269
REBO	154.361	45.760	54.299	140.796	0.296
SW16	133.025	39.386	46.821	121.364	0.296
ReaxFF	230.119	115.693	57.135	171.954	0.503

Table S4. The elastic constants C_{11} of monolayer MoS_2 with a line defect and single point vacancies defects with 1, 2 and 3 sulfur vacancies calculated by DFT and MD with different interatomic potentials.

Potential	Point_1	Point_2	Point_3	Line_2	Line_3
DFT	128.657	124.367	120.877	126.079	124.054
SW13	80.846	79.918	79.064	80.239	79.632
SW13_f	137.734	134.770	132.249	135.680	133.746
SW15	101.237	97.358	94.304	98.837	96.719
REBO	150.087	145.980	142.894	147.744	163.409
SW16	129.118	125.469	122.382	126.672	124.406
ReaxFF	255.420	268.222	248.998	4191.688	-19290.578

Table S5. The elastic constants C_{12} of monolayer MoS_2 with a line defect and single point vacancies defects with 1, 2 and 3 sulfur vacancies calculated by DFT and MD with different interatomic potentials.

Potential	Point_1	Point_2	Point_3	Line_2	Line_3
DFT	33.539	33.056	32.274	32.169	30.772
SW13	29.766	29.367	28.968	29.332	28.885
SW13_f	51.358	50.056	48.832	49.842	48.366
SW15	26.886	25.633	24.433	25.133	23.390
REBO	44.680	43.819	42.748	42.887	1.667
SW16	38.184	37.049	36.081	36.957	35.781
ReaxFF	98.136	125.731	75.249	1414.225	4707.022

Table S6. The elastic constants C_{22} of monolayer MoS_2 with a line defect and single point vacancies defects with 1, 2 and 3 sulfur vacancies calculated by DFT and MD with different interatomic potentials.

Potential	Point_1	Point_2	Point_3	Line_2	Line_3
DFT	128.496	124.479	119.497	122.130	114.611
SW13	80.842	79.912	79.033	79.945	79.032
SW13_f	137.724	134.721	131.937	134.301	130.864
SW15	101.207	97.214	93.499	95.703	89.739
REBO	150.021	145.862	141.738	142.913	107.420
SW16	129.155	125.296	122.017	125.188	121.380
ReaxFF	222.711	264.662	208.454	-5970.110	-567.385

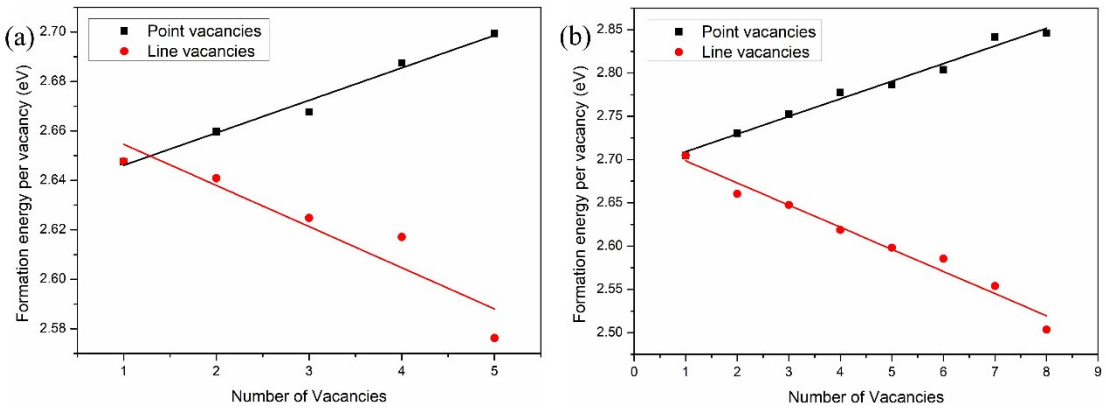

Figure S1. The formation energy per sulfur vacancy of monolayer MoS_2 with single sulfur point vacancies and line vacancies defects with different numbers of vacancies obtained from (a) First principles, (b) Molecular dynamics.

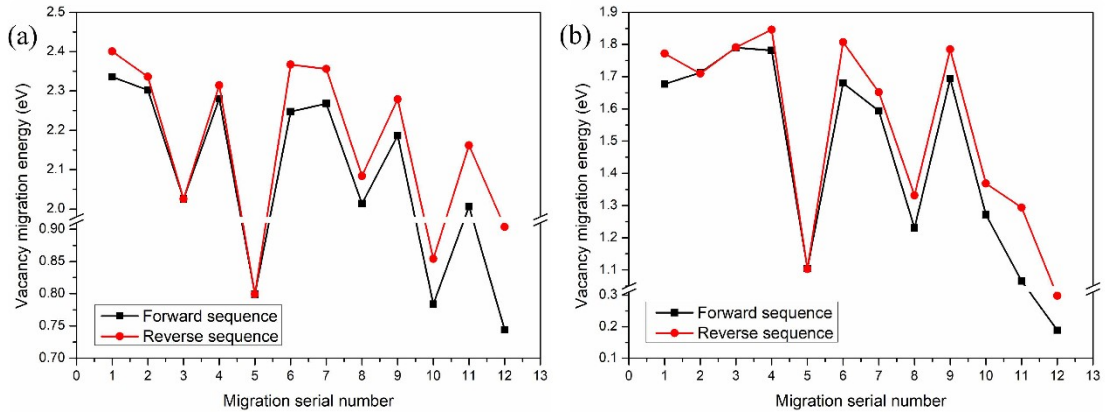

Figure S2. Sulfur vacancy migration energy in monolayer MoS_2 obtained from (a) First principles, (b) Molecular dynamics.

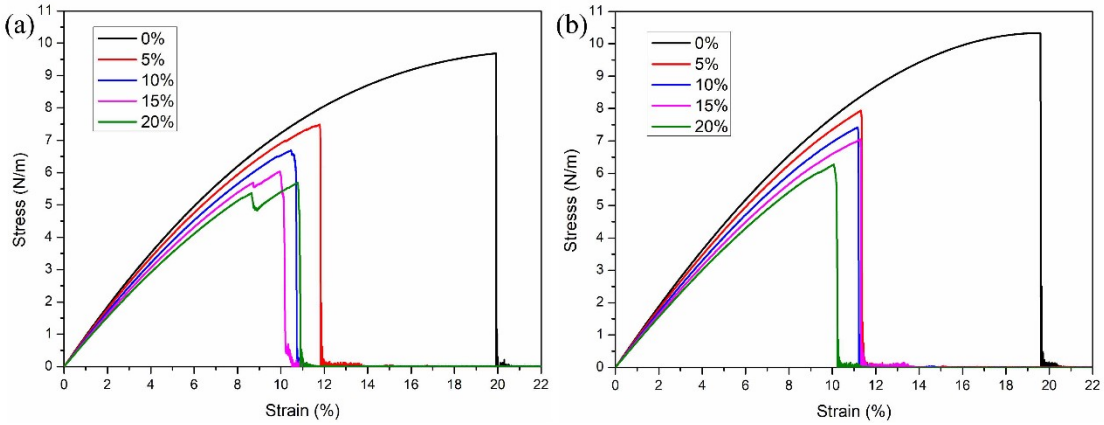

Figure S3. The stress–strain curves of monolayer MoS_2 with different single sulfur vacancy concentrations before the defect evolution in (a) zigzag direction and (b) armchair direction.

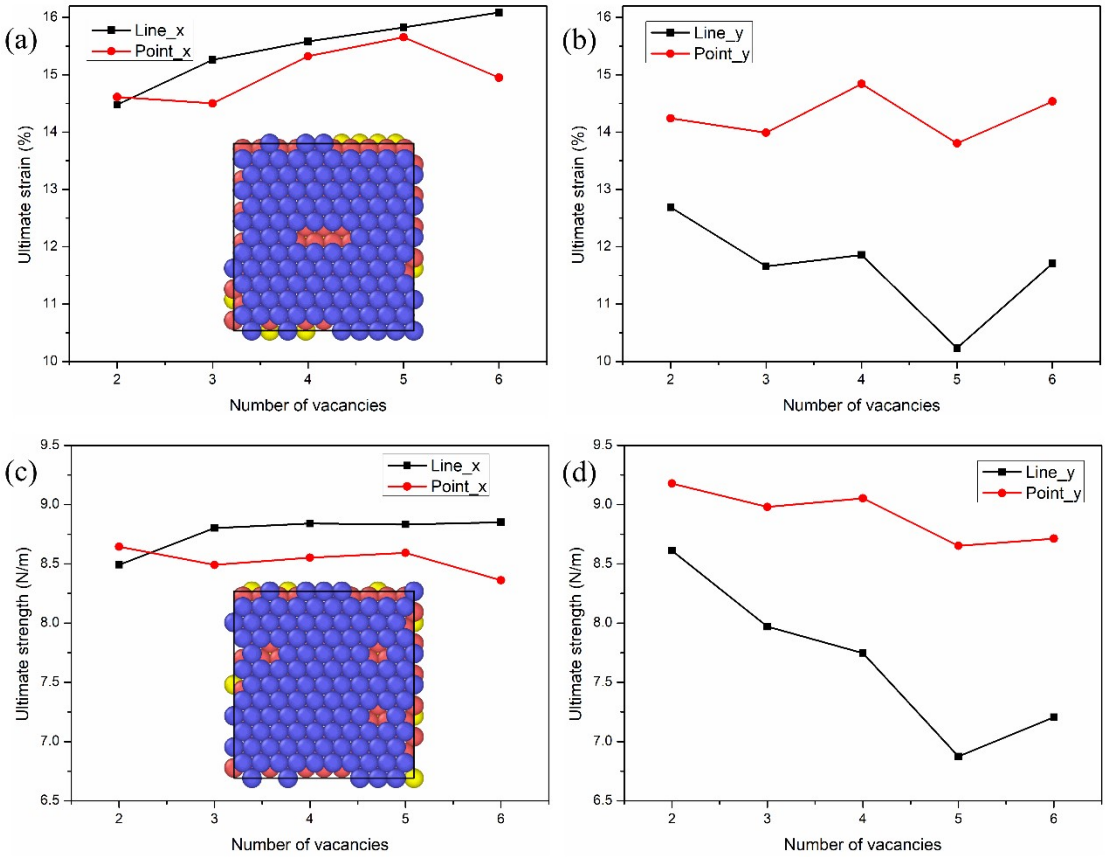

Figure S4. The (a, b) ultimate strain and (c, d) ultimate strength of monolayer MoS_2 with a line vacancies defect along x zigzag direction and single point vacancy defects with the same number of sulfur vacancies under uniaxial tensile loading along the (a, c) x zigzag and (b, d) y armchair direction.

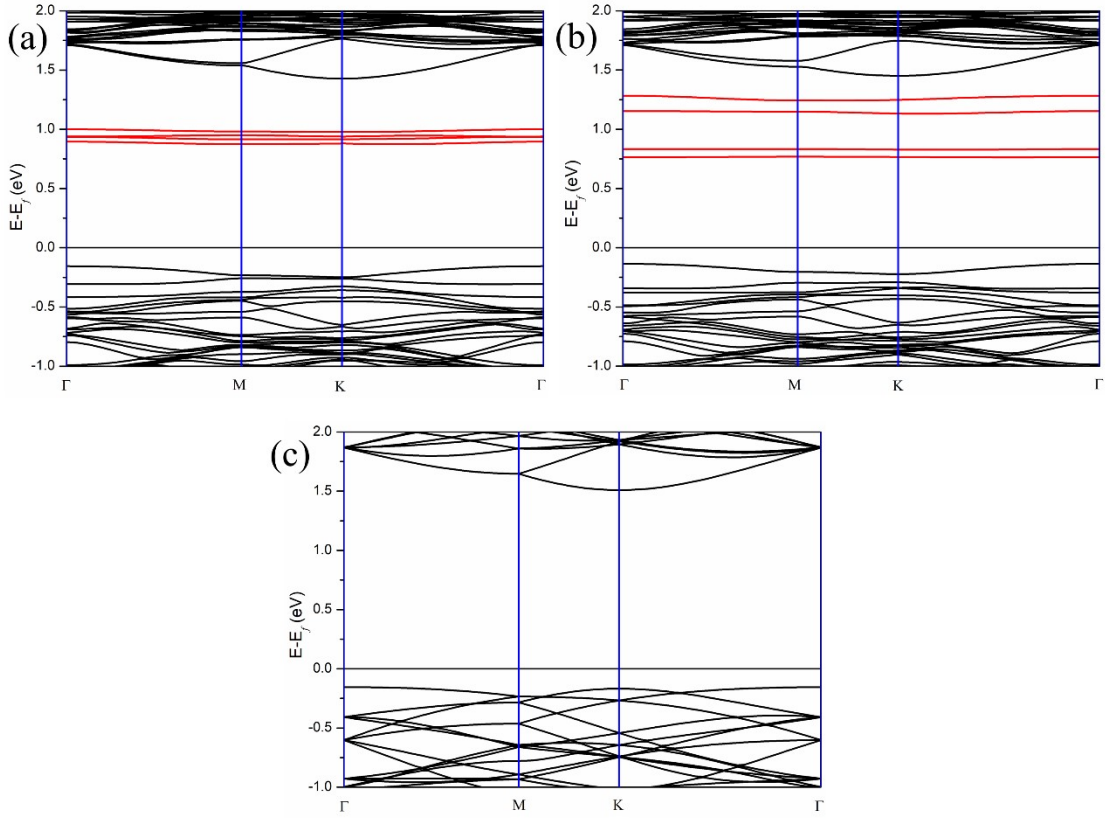

Figure S5. Calculated electronic band structures of monolayer MoS_2 with (a) two single sulfur vacancies, (b) di-vacancy line defect, and (c) pristine monolayer MoS_2. The defective states are denoted by red lines. The Fermi level is set to zero.

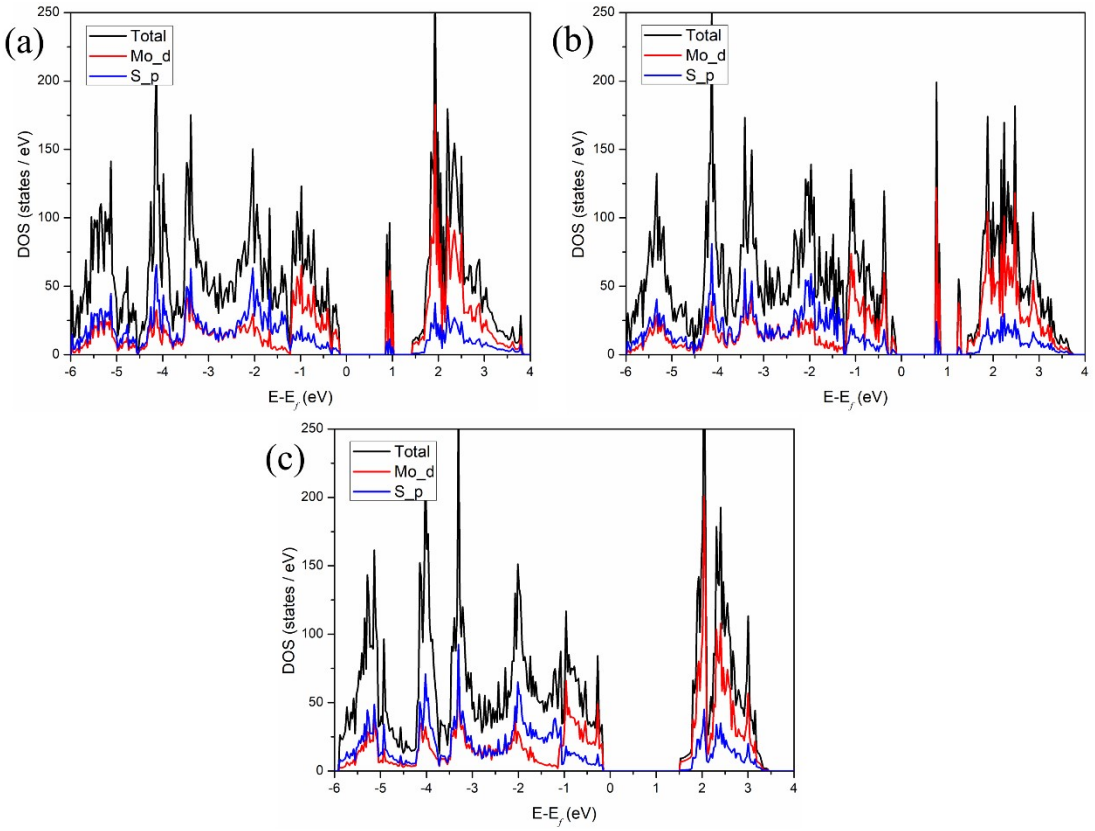

Figure S6. Total density of states (DOS) and partial DOS of monolayer MoS_2 with (a) two single sulfur vacancies, (b) di-vacancy line defect, and (c) pristine monolayer MoS_2. The Fermi level is set to zero.

References:

[1] M. Wen, S.N. Shirodkar, P. Plecháč, E. Kaxiras, R.S. Elliott, E.B. Tadmor, A force-matching Stillinger-Weber potential for MoS2: Parameterization and Fisher information theory based sensitivity analysis, Journal of Applied Physics, 122 (2017) 244301.

[2] Y. Han, T. Hu, R. Li, J. Zhou, J. Dong, Stabilities and electronic properties of monolayer MoS2 with one or two sulfur line vacancy defects, Physical Chemistry Chemical Physics, 17 (2015) 3813-3819.

[3] S. Kc, R.C. Longo, R. Addou, R.M. Wallace, K. Cho, Impact of intrinsic atomic defects on the electronic structure of MoS2 monolayers, Nanotechnology, 25 (2014) 375703.

[4] S. Thomas, K.M. Ajith, M.C. Valsakumar, Directional anisotropy, finite size effect and elastic properties of hexagonal boron nitride, Journal of Physics: Condensed Matter, 28 (2016) 295302.